Available online at www.sciencedirect.com
SCIENCE DIRECT
Spectrochimica Acta Part A 63 (2006) 130–138
SPECTROCHIMICA ACTA PART A
www.elsevier.com/locate/saa

SOM assembly of hydroxynaphthoquinone and its oxime: Polymorphic X-ray structures and EPR studies

Ashwini V. Todkary [a], Rupali Dalvi [a], Sunita Salunke-Gawali [b], Jorge Linares [b], François Varret [b], Jérôme Marrot [c], Jatinder V. Yakhmi [d], Mohan Bhadbhade [e], D. Srinivas [e], Shridhar P. Gejji [a], Sandhya Y. Rane [a,*]

[a] *Department of Chemistry, University of Pune, Pune 411007, India*
[b] *Laboratoire de Magnétisme et d'Optique, CNRS, UMR 8634, Université de Versailles, 45 Avenue des Etats-Unis, 78 035 Versailles Cedex, France*
[c] *Institut Lavoisier, IREM, CNRS, UMR 8637, Université de Versailles, 45 Avenue des Etats-Unis, 78 035 Versailles Cedex, France*
[d] *Technical Physics & Prototype Engg. Division, Bhabha Atomic Research Centre, Trombay, Mumbai 400085, India*
[e] *National Chemical Laboratory, Pune 411008, India*

Received 4 March 2005; accepted 26 April 2005

Abstract

Investigation on solvent-induced polymorphism in X-ray structures of 2-hydroxy-1,4-naphthoquinone (Lawsone) **1**, is carried out. In protic methanol, **1** crystallizes in monoclinic space group $P2_1/c$ (**1a**) comprising of 2D hydrogen bonded network via cyclic dimers. In aprotic solvent such as acetone on the other hand, **1** exhibits orthorhombic space group $Pna\,2_1$ (**1b**) and emerges with 1D catemeric chain. Solvent-induced topological isomerism of cyclic dimers and helical catemeric chains arising from (i) bifurcated intra- and inter molecular hydrogen bondings viz. O─H···O═C interactions between C(2) hydroxyl and C(1), C(4) carbonyls, (ii) C─H···O interactions viz. C(3)─H···O(1)C(1) have been discussed. A signal for radical in **1** at $g = 2.0058$ is signatured by EPR spectrum and it's oxime derivative viz. 2-hydroxy-4-naphthoquinone-1-oxime **2**, in solid state shows biradical and monoradical formation with aggregation of dimer and monomer due to non-covalent hydrogen bonds. Zero field split parameters for **2** are estimated to be $D = 215$ G, $E_x = 13$ G, $E_y = 47$ G at 298 K. A half field signal at 77 K indicates triplet ground state. Frozen glass EPR of **2** resolves as regioregular dimeric–monomeric species showing hyperfine interactions with 1-oximino nitrogen in dimer $\bar{A}(^{14}N) = 15.5$ G].

Keywords: Hydroxy naphthosemiquinone; Bifurcated hydrogen bonding; Self organized molecular assembly (SOM); Biradicals; Lawsone

1. Introduction

Self organized molecular assembly (SOM) leads to crystal engineering in coordination polymers of hydroxy-naphthoquinones through directional non-covalent hydrogen bonds [1–2]. Henna, viz. 2-hydroxy-1,4-naphthoquinone commonly known as Lawsone **1**, a naturally occurring spin carrier compound possesses tremendous potential as chemo-taxonomic marker in biology [3], as an electron transfer mediator in chemical fuel cells in chemistry [4–5] and as molecular magnetic materials in physics [6–7]. The oxime derivative of **1**, viz. 2-hydroxy-4-naphthoquinone-1-oxime **2** performs functional dimeric manganese model of water oxidizing complex in PS-II [8,9].

In present paper, we report the supramolecular hydrogen bonding networks induced by different protic and aprotic solvents leading to polymorphic behavior in **1**. Also we discuss the capability of **1** as an intrinsic neutral radical ligand due to formation of hydrogen bonded chains in its crystal structures. We have already reported hydrogen bonding route that carries electron density on an end or terminal molecule [10] which may give rise to radical ligation in **1** [11]. The distinguished feature of 2-OH and 1-oximino functions in **2**, exhibiting '*syn*', '*anti*' and '*amphi*' conformers [12] are due to intra- as well as intermolecular hydrogen bonding which was recently

* Corresponding author. Fax: +91 20 25691728.
E-mail address: syrane@chem.unipune.ernet.in (S.Y. Rane).

1386-1425/$ – see front matter © 2005 Elsevier B.V. All rights reserved.
doi:10.1016/j.saa.2005.04.054

investigated by us theoretically using the Hartree Fock (HF) and density functional theory (DFT) [13]. With this view in present work, the EPR signatures of **2** are discussed in relation to its molecular association tendency via hydrogen bonded interactions revealing the possibility of **2** as a radical ligand.

2. Experimental

1 was obtained from Sigma and was used as received. Single crystals were grown from solutions by cooling. Solvents employed were methanol and acetone purchased from Qualigens fine chemicals and purified according to the literature procedure [14]. 2-Hydroxy-4-naphthoquinone-1-oxime, **2** was prepared according to procedure reported earlier [15]. The X-band powder and frozen glass EPR spectra were recorded on Varian E-4 EPR spectrometer employing 100 kHz field modulation using TCNE as the g-marker. The crystal structures were solved for the crystals **1a** and **1b** at Université de Versailles, France.

2.1. X-ray crystallography

An orange crystal, 0.28 mm × 0.24 mm × 0.04 mm for **1a** and a brown crystal, 0.50 mm × 0.12 mm × 0.04 mm for **1b** were glued to a glass fibre. Intensity data were collected at room temperature with a Siemens SMART diffractometer equipped with a CCD two-dimensional detector [λ Mo Kα = 0.71073 Å]. Slightly more than one hemisphere of data was collected in 1271 frames with ω scans (width of 0.30° and exposure time of 30 s per frame). Data reduction was performed with SAINT software. Data were corrected for Lorentz and polarization effects, and a semi-empirical absorption correction based on symmetry equivalent reflections was applied by using the SADABS program [16]. Lattice parameters were obtained from least-squares analysis of all reflections. The structure was solved by direct method and refined by full matrix least-squares, based on F^2, using the SHELX-TL software package [17]. All non-hydrogen atoms were refined with anisotropic displacement parameters. All hydrogen atoms were located with geometrical restraints in the riding mode.

3. Results and discussion

3.1. Polymorphic X-ray crystal structures of 1

The single crystal X-ray structure of Lawsone **1** is solved in two different crystal forms obtained from respective solvents. A summary of crystallographic data for dimorphs of **1** are recorded in Table 1.

The orange crystals of **1** crystallized from methanol (protic solvent) belong to the monoclinic space group $P2_1/c$ (form **1a**) whereas brown crystals of **1** obtained from acetone (aprotic solvent) belongs to the space group $Pna2_1$ (form **1b**).

Table 1
Summary of crystallographic data for **1a** and **1b**

Compound	**1a**	**1b**
Empirical formula	C_{30} H_{18} O_9	C_{20} H_{12} O_6
Formula weight	522.44	348.30
Temperature (K)	296 (2)	296 (2)
Wavelength (Å)	0.71073	0.71073
Crystal system, space group	Monoclinic, $P2_1/c$	Orthorhombic, $Pna2_1$
a (Å)	9.5438 (3)	16.899 (10)
b (Å)	12.5931 (4)	3.828 (2)
c (Å)	19.9763 (5)	12.056 (10)
α (°)	90	90
β (°)	99.471 (1)	90
γ (°)	90	90
Volume (Å^3)	2368.15 (12)	780.0 (9)
Z	4	2
Calculated density (mg m^{-3})	1.465	1.483
Absorption coefficient (mm^{-1})	0.110	0.111
F (0 0 0)	1080	360
Theta range for data collection (°)	1.92–23.30	2.41–29.83
Limiting indices	$-8 \le h \le 10$, $-13 \le k \le 14$, $-21 \le l \le 22$	$-12 \le h \le 19$, $-5 \le k \le 5$, $-6 \le l \le 16$
Reflections collected/unique	10491/3411 [R(int) = 0.0536]	2429/1144 [R(int) = 0.0553]
Completeness to theta = 23.30 (%)	99.7	84.9
Absorption correction	None	SADABS
Refinement method	Full-matrix least-squares on F^2	Full-matrix least-squares on F^2
Data/restraints/parameters	3411/0/356	1144/1/119
Goodness-of-fit on F^2	1.053	1.123
Final R indices [$I > 2$sigma(I)]	$R1 = 0.0576$, $wR2 = 0.1231$	$R1 = 0.0761$, $wR2 = 0.1755$
R indices (all data)	$R1 = 0.1100$, $wR2 = 0.1466$	$R1 = 0.1087$, $wR2 = 0.1977$
Absolute structure parameter	0.0013 (4)	4 (3)
Largest diff. peak and hole (Å^{-3})	0.172 and −0.183	0.367 and −0.220

The effect of solvents on different nucleation pathways has been the subject of intensive investigations [18], therefore controlling the nucleation of the desired polymorph is one of the main objectives in case of pharmaceutical solids like **1** [3]. There are mainly three types of the hydrogen bondings observed in 1D and higher dimensional structures of **1** viz. (i) intermolecular hydrogen bonding between O(2)–H···O(3) and (ii) an intramolecular hydrogen bonding between O(2)–H···O(1). A "bifurcated" hydrogen bonding had been reported by Gaultier and Hauw in C(3) methyl derivative (phthiocol) [19] and in C(3) chloro derivative of **1** [20] and (iii) intermolecular hydrogen bonding interaction is observed between C(3)H···O(1) [2]. There is also a third polymorph of **1** reported earlier by Dekkers et al. [21] which was crystallized from acetonitrile in triclinic space group $P\bar{1}$ (hereafter form **1c**). Thus, an apparently rigid molecule Lawsone **1**, till to date, is known to exist in three polymorphic modifications due to the differences in the intermolecular interactions brought about essentially by the solvent used in crystallization. The bond distances, bond angles and torsion angles for the forms **1a** and **1b** are recorded and are deposited as a supplementary material.

Interestingly, the forms **1a**, **1b** and **1c** contain three, one and two molecules in their asymmetric units, respectively. Fig. 1 displays a typical ORTEP [22] view of a single molecule exhibiting intra molecular O(2)–H(2)···O(1) hydrogen bonding, with ∠OHO ∼115°, in all the three polymorphs. The atomic numbering in the crystal structures are modified according to IUPAC and are consistent with the numbering deposited with the Cambridge Crystallographic Data Centre. The hydrogen bonding parameters are given in Table 2. Molecular packing for **1a** and **1b** are shown in Fig. 2. Hydroxyl group O(2)–H(2) in **1a** and **1b** makes a bifurcated hydrogen bond; apart from the intra molecular interaction, it also makes another intermolecular hydrogen bond with the carbonyl oxygen O(3) in all the three forms. However, the relative orientations of the neighboring molecules in form **1b** are quite different from those in **1a** and **1c** but

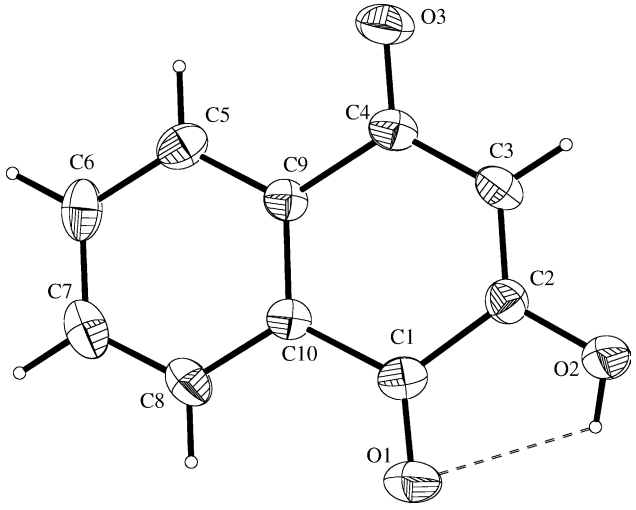

Fig. 1. ORTEP view of **1b** with atom numbering. Intra molecular O—H···O bonding common in all forms of **1** is displayed.

the latter two are similar. As mentioned earlier, form **1a** is comprised of three molecules in the asymmetric unit where planar layers of molecule B are sandwitched between two layers of molecules of A–C on either side. It is noteworthy that each layer, either A–C–A–C··· or B–B–B··· has the same architecture as shown in Fig. 2. Molecules in form **1a** (and also reported form **1c**) assemble to form planar 'molecular tapes' linked by two bridging interactions O(2)–H(2)···O(3) and O(1)···H(3)–C(3) between the two neighboring molecules (Fig. 3), it's only that their stacking in the third dimension with different degree of overlap makes them distinct. But in a different assembly of form **1b**, single molecule makes O(2)–H(2)···O(3) bridge with one molecule and O(1)···H(3)–C(3) interaction with the second (unit translated) molecule (Fig. 4). The basic difference in the polymorphs **1a** and **1b** arises from this difference in their topologies of hydrogen bonding interactions. Referring to Fig. 3 and Fig. 4 geometries of these interactions show significant differences; intermolecular O(2)–H(2)···O(3)

Table 2
Hydrogen bonding parameters for **1a** and **1b**

D H A	Symmetry	D—H (Å)	H···A (Å)	D···A (Å)	∠D—H···O (°)
Form **1a**[a]					
O(2A)—H(2A)···O(1A)	(i)	0.82	2.21	2.675	116
O(2A)—H(2A)···O(3C)	(ii)	0.82	2.01	2.712	143
O(2B)—H(2B)···O(1B)	(i)	0.82	2.22	2.673	115
O(2B)—H(2B)···O(3B)	(iii)	0.82	2.01	2.703	143
O(2C)—H(2C)···O(1C)	(i)	0.82	2.22	2.676	115
O(2C)—H(2C)···O(3A)	(ii)	0.82	2.04	2.734	143
C(3A)—H(3A)···O(1C)	(iv)	0.93	2.51	3.333	147
C(3B)—H(3B)···O(1B)	(v)	0.93	2.51	3.327	147
C(3C)—H(3C)···O(1A)	(vi)	0.93	2.50	3.295	144
Form **1b**[b]					
O(2)—H(2)···O(1)	(i)	0.82	2.22	2.676	116
O(2)—H(2)···O(3)	(ii)	0.82	2.02	2.684	136
C(3)—H(3)···O(1)	(ii)	0.93	2.67	3.526	152

[a] Symmetry code: (i) = x, y, z; (ii) = $2-x, 1/2+y, 1/2-z$; (iii) = $-x, -1/2+y, 1/2-z$; (iv) = $2-x, -1/2+y, 1/2-z$; (v) = $-x, 1/2+y, 1/2-z$.
[b] Symmetry code: (i) = x, y, z; (ii) = $1/2-x, -1/2+y, 1/2+z$.

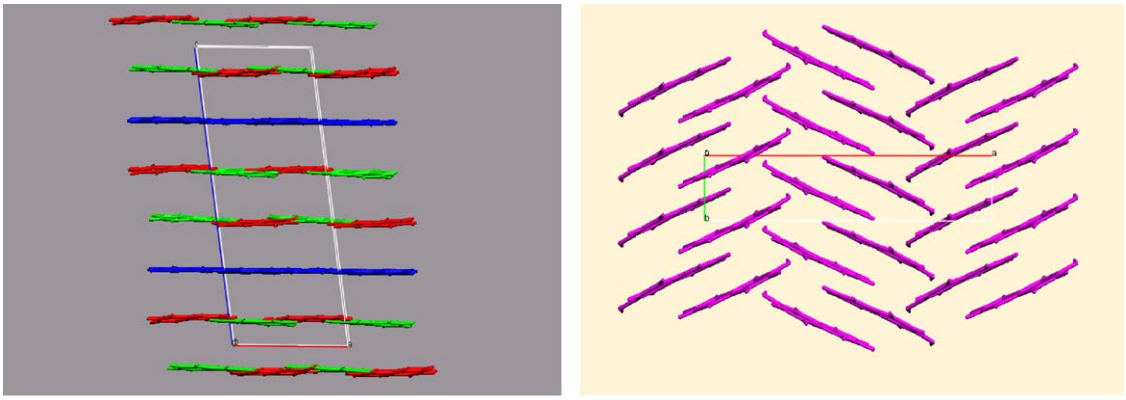

Form 1a Form 1b

Fig. 2. Packing of molecules in **1a** (down *b*-axis) and **1b** (down *c*-axis).

in form **1b** has the shortest D···A distance (2.684 Å) compared to the observed distances in form **1a** (2.703 Å and 2.734 Å) but the deviation from linearity is larger in form **1b** (∠O(2)–H(2)···O(3) = 138°) compared to that in **1a** (∠143°). The elongation of C(3)–H(3)···O(1) interactions in **1b** (2.67 Å, ∠152°) compared to **1a** (2.50 Å, ∠144° in A–C···layer and 2.51 Å, ∠147° in B–B···layer) could lead to disruption in the formation of planar molecular tapes in **1b**. Such disruption may be due to the presence of two hydrophobic methyl groups of acetone (solvent used for crystallization), which may break the dimerization in plane leading to herring bone pattern in **1b**.

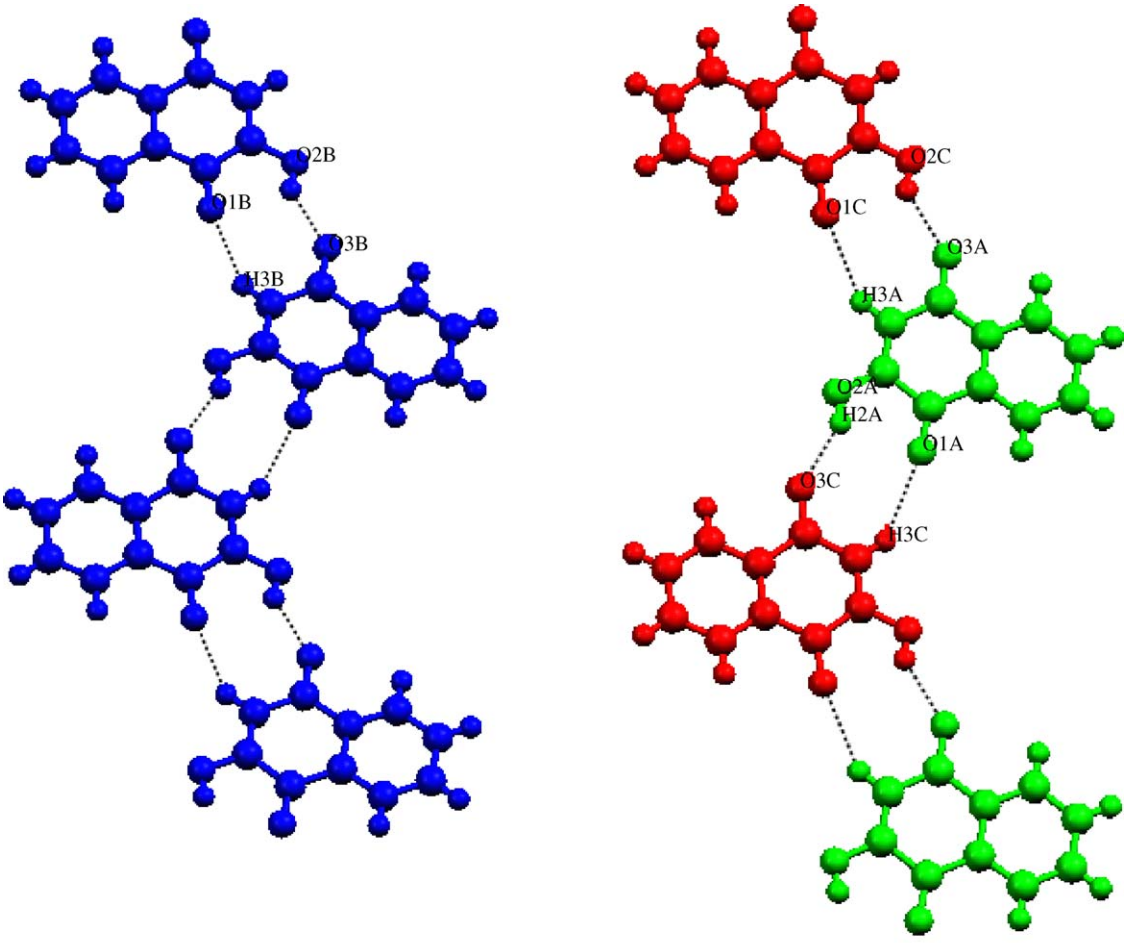

(i) B-B-B---layers (ii) A-C--- layers

Fig. 3. (i) Molecular tapes of **1a** for B─B─B··· layer. (ii) Molecular tapes of **1a** for A─C··· layer.

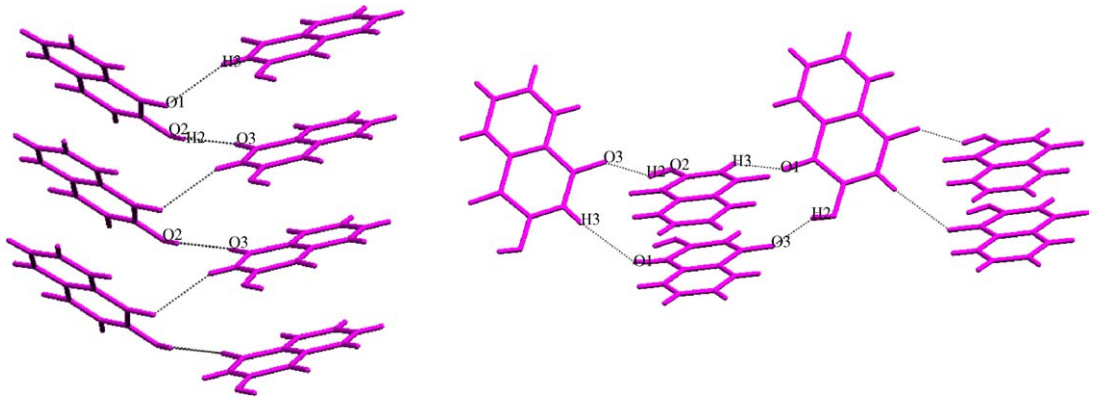

(i) Molecular tapes of **1b** as herring bone pattern. **(ii)** Molecular tapes of **1b** with unit translated C–H---O interaction.

Fig. 4. (i) Molecular tapes of **1b** as herring bone pattern. (ii) Molecular tapes of **1b** with unit translated C—H···O interaction.

Although polymorphs **1a** and reported **1c** are isostructural [23], they differ in two dimensions with respect to the extent of overlapping of the neighboring layers. Whereas basic difference between form **1a** and **1b** arises from the absence of π–π stacking in **1a** despite interplanar separation (∼3.6 Å) and presence of slipped π–π stacking [24] (cf. Fig. 4(ii)) between the unit translated molecules on 2_1 screw axis as 3.828 Å in **1b**.

3.2. *The intrinsic semiquinone radicals in **1** and **2***

It's well known fact that the semiquinone radicals in naphthoquinones are generated by chemical oxidation/reduction of naphthols or naphthoquinones in alkaline medium [25–29]. Recently Pedersen has reported the semiquinone radicals [30] of *para*- and *ortho*-hydroquinones at physiological pH in buffered solutions under continuous access of molecular oxygen and declared that there is no requirement of alkaline high pH and reactions induced by OH^- ions in unsubstituted quinonoidal naphthoquinones may be contributing in generation of semiquinone radical.

In the supra X-ray structural discussion we have shown that the SOM assembly formation of Lawsone **1** is due to bifurcated hydrogen bonding. The reports on theoretical molecular modeling of **1** with respect to monomeric tautomers [31] influenced by solvent polarity [32] emphasize the significance of 2-hydroxyl group in monomeric tautomerism of **1**. Our recent investigations on the energetics and charge

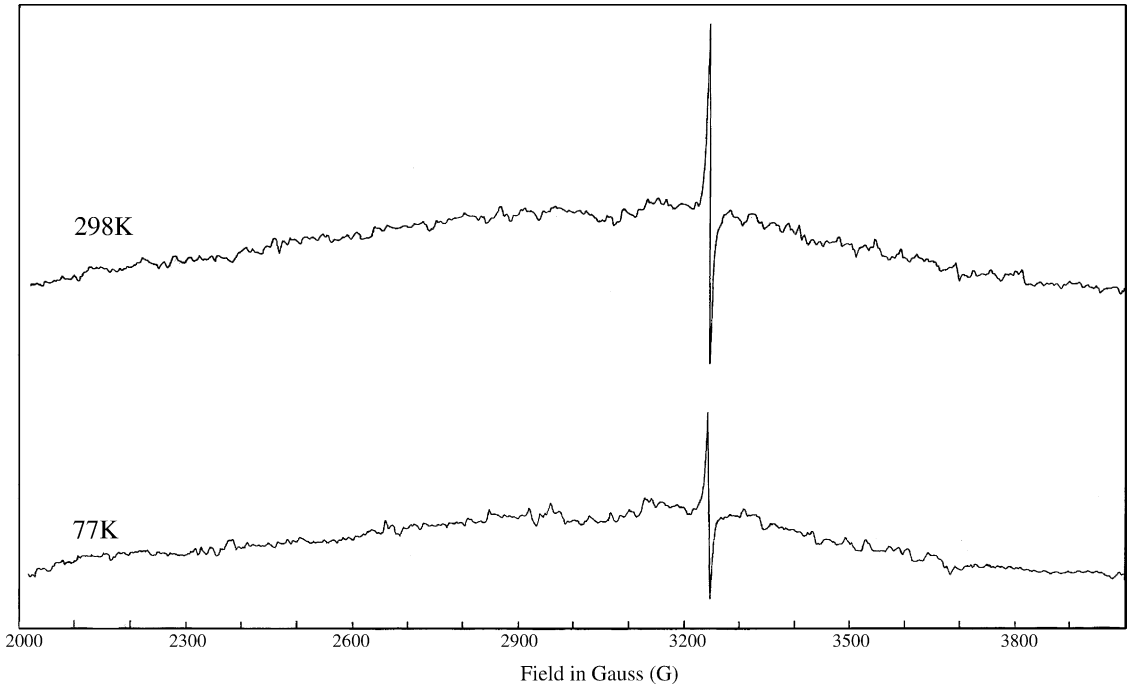

Fig. 5. (a) Solid state EPR spectrum of **1** at 298 K. (b) Solid state EPR spectrum of **1** at 77 K.

distribution in polymeric molecular system of **1** [10] reveals the percolation of electron density through intermolecular hydrogen bonding on end carbonyl of *para*-position so that **1** may perform a 2-hydroxy-1,4-naphthosemiquinone species intrinsically without any chemical reduction of 2-hydroxy-naphthoquinone. It is clearly signatured by EPR spectral line at $g = 2.0058$ at 298 K and at 77 K spectra (cf. Fig. 5(a) and (b)). Since these signals do not show any hyperfine splits we haven't taken an expanded spectrum because the literature is flooded with EPR of semiquinone radicals generated chemically and electrochemically or by catalytic routes using complexes [25–30,33–36]. Here, we want to infer that the hydrogen bonding effect performing SOM assembly of **1**, may be the driving force in forming a stable neutral radical intrinsically in nature. To confirm this we have derivatized **1** as oxime, **2** viz. 2-hydroxy-4-naphthoquinone-1-oxime. The solid state EPR spectra of **2** at 298 K and 77 K together with frozen glass EPR in methanol are shown in Fig. 6(a)–(c), respectively.

A seven line solid state ESR spectrum of **2** at 298 K (cf. Fig. 6(a)) is characteristic for regiorandomly oriented triplet system of biradicals with $E \neq 0$ and monoradical of *para*-naphthosemiquinone species. The magnetic parameters for dimeric $S = 1$ species and strong monomeric monoradical $S = 1/2$ species at $g_{iso} \sim 2$ signal are presented in Table 3. The solid state spectrum of **2** (cf. Fig. 6(b)) at 77 K exhibits both

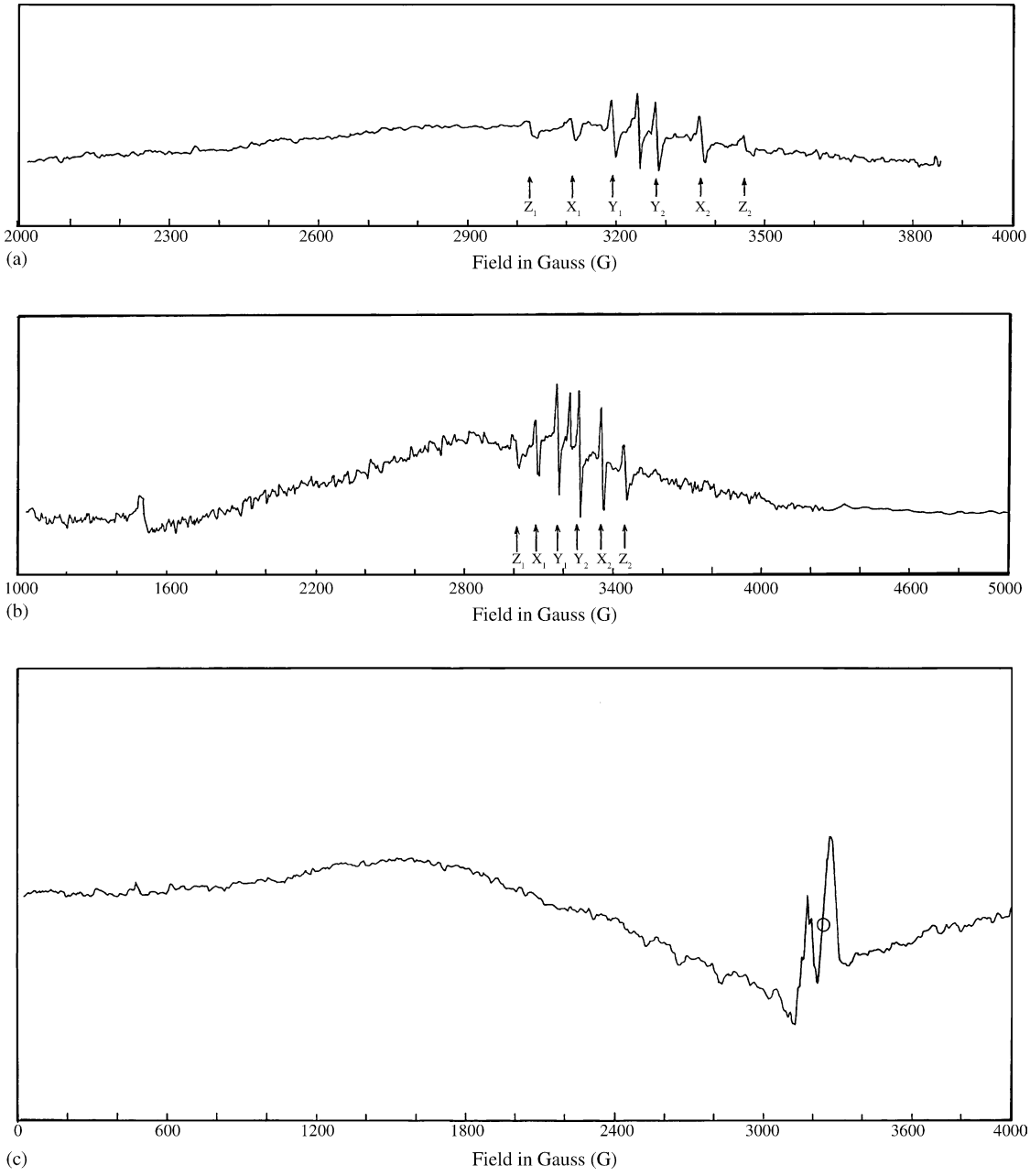

Fig. 6. (a) Solid state EPR spectrum of **2** at 298 K. (b) Solid state EPR spectrum of **2** at 77 K. (c) Frozen glass EPR spectrum of **2** in methanol at 77 K.

Table 3
Magnetic parameters of $S = 1$ and $S = 1/2$ species in **1** and **2**

Compound	Temperature (K)	Physical state	g-factors	D (G)	E (G)	$\bar{A}(^{14}N)$ (G)
1	298	Solid	2.0058	–	–	–
	77	Solid	2.0058	–	–	–
2	298	Solid	$\bar{g}_x = 2.0025$ $\bar{g}_y = 2.0015$ $\bar{g}_z = 2.0095$	215	47 (y) 13 (x)	
	77	Solid	$\bar{g}_x = 1.9768$ $\bar{g}_y = 1.9798$ $\bar{g}_z = 1.9893$	250		
	77	Frozen glass in methanol	$g_1 = 2.0619$ $g_2 = 1.9773$			$\bar{A} = 15.5$

typical fine structure in the $\Delta m_s = \pm 1$ region and show weak $\Delta m_s = \pm 2$ transition as half field signal at 1515G indicating high spin ($S > 1/2$) as triplet ground state. We have assigned the signals of EPR spectrum recorded at 298 K (marked with arrows in Fig. 6(a)) for $H_{||z}$, $H_{||x}$ and $H_{||y}$ transitions of high spin species [37–38] in $\Delta m_s = \pm 1$ region. A strong signal at 3253 G is due to free neutral monoradical with $S = 1/2$ species coupled from double quantum transitions. The zero field split parameters D and E are estimated from field positions of anisotropic g factors [37] such as $D = 215$ G (0.0200 cm^{-1}) and $E_y = 47$ G (0.0043 cm^{-1}) and $E_x = 13$ G (0.0012 cm^{-1}). A frozen glass EPR spectrum of **2** in protic methanol confirms the presence of equivalent iminoxy biradicals. Those may be formed analogous to cyclic dimer of parent ligand **1** together with hydrogen bonded monomer as shown in Fig. 3. Thus three rotamers give rise to two main signals at $g_1 = 2.0619$ and $g_2 = 1.9773$. Signal at lower field exhibits hyperfine split interaction of radical with two ^{14}N nuclei of iminoxy nitrogen in dimers of **2** so that five splits with $\bar{A}(^{14}N)$ as 15.5 G is resulted. This cyclic equivalent biradical may be formed in A–C layered molecules on 2_1 rotational axis analogous to supra form **1a** (Fig. 3) in methanol. Localized electron densities on these two end molecules via inter- and intra molecular hydrogen bondings of middle molecule leads to hyperfine split interaction. In A–C layered molecules planarity is slightly disturbed however second signal is broad with nearly same band width of former signal but devoid of hyperfine splits. This monoradical signal may be due to hydrogen bonded layer of B molecules analogous to **1a** as shown in Fig. 3 in which the electron density may not be localized as a result of total planarity. There is possibility of fast percolation of electron density through "molecular tapes" in planar B–B layer. Hence, oligomers of oxime **2** may become regioregular type in methanolic frozen glass matrix analogous to parent Lawsone **1a** polymorph in methanol.

3.3. Correlation of magneto structures of *1* and *2* with X-ray crystal structures

Finally we can conclude that the spin transfers in **2** via iminoxy biradicals and monoradical based on its proposed structural correlation with parent ligand **1a** (crystallized from protic solvent). Using the spin model in which the spins are localized on iminoxy nitrogen in cyclic dimer of **2** the separation distance R is calculated as 5.05 Å from spin–spin interaction D [34,39,40] between radicals compared to the Cu^{+2}–Cu^{+2} distance (5.03 Å) which is reported in supramolecularly hydrogen bonded copper complex of **1** viz., $[Cu(II)(ONQ)_2(H_2O)_2]_n$ obtained from methanol [2]. Table 4 shows the C–O bond distances for *p*-ONQ (2-oxido-1,4-naphthoquinone) ligand molecule from X-ray structure of copper(II) complex [41] which are compared with **1a**

Table 4
Comparison of bond distances in respective helix of molecular tapes in **1a**

[a](p) C═O	C—O	Quinone (Q) 1.216[b]	Semiquinone (SQ) 1.27–1.30[c]	Catechol (CAT) 1.34–1.36[d]
[a](p) C_{4B}—O_{3B}[e]		–	1.232 (B)[a,e]	–
[a](p) C_{4C}—O_{3C}[e]		–	1.234 (C)[a,e]	–
	C_{2B}—O_{2B}[e]	–	–	1.339 (B)[e]
	C_{2C}—O_{2C}[e]	–	–	1.331 (C)[e]
C_{4C}—O_{3C}[f,g]		1.222[f]	–	–
		1.236[g]	1.255[g]	–

[a] (p)—*para* position.
[b] [41].
[c] [44].
[d] [45].
[e] Present investigation.
[f] [43].
[g] [34].

structure of ligand. The C–O bond distances for hydrogen bonded *para*-carbonyls show increase in bond lengths by ∼0.016 Å and 0.018 Å in respective helix of molecular tapes in **1a**. McGarvey and coworkers [34] has reported similar increase in *para*-carbonyl function in Li^+ (*p*-semiquinone) as shown in Table 4. The C_{2B}–O_{2B} and C_{2C}–O_{2C} bond distances in two types of molecular tapes viz. A–C··· and B–B··· in **1a** are equivalent to catechol function confirming the presence of 2-hydroxy-1,4-naphthosemiquinone form and not 4-hydroxy-1,2 naphthoquinone form of the ligand **1** [42].

4. Conclusions

Self organized molecular assemblies of Lawsone **1**, are induced by protic (methanol) and aprotic (acetone) solvents which result in two polymorphs viz. **1a** and **1b**. Through intermolecular hydrogen bonding electron density percolates in molecular tapes leading to intrinsic radical formation in parent ligand **1** as well as in its oxime derivative **2**. Since **2** is obtained from protic methanol, it shows 'ABC' type supramolecular magnetostructure similar to X-ray structure of form **1a**. The structural analogy of **1a** with **2**, such as cyclic dimers on 2_1 rotational axis of 'A–C' type molecules and 'B' type planar layered molecules is investigated from EPR signatures of biradicals and monoradical in regioregular hydrogen bonded molecular tapes.

Supporting information available

Crystallographic data of **1a** and **1b** have been deposited with the Cambridge Crystallographic Data Centre and may be obtained on request quoting the deposition number CCDC-215003 and 215004, respectively from the CCDC, 12 Union Road, Cambridge CB21EZ, UK. Torsion angles, bond distances and bond angles are deposited as supplementary material (Fax: +44 1223 336 033; E-mail address: deposit@ccdc.cam.ac.uk).

Acknowledgements

SYR is grateful to the CSIR, New Delhi, India (01(1686)/00/EMR-II) for the Grant. AVT is thankful to Department of Atomic Energy, Govt. of India for providing research fellowship through collaborative scheme of Bhabha Atomic Research Centre (BARC) with Pune University. SSG is thankful to the Indo-French seminar (Bangalore 2000) for providing a meeting opportunity to the French government for post doctoral fellowship.

Appendix A. Supplementary data

Supplementary data associated with this article can be found, in the online version, at doi:10.1016/j.plantsci.2004.08.011.

References

[1] P. Garge, R. Chikate, S. Padhye, J.-M. Savariault, P. de Loth, J.P. Tuchagues, Inorg. Chem. 29 (1990) 3315–3320.
[2] S. Salunke-Gawali, S.Y. Rane, V.G. Puranik, C. Guyard-Duhayon, F. Varret, Polyhedron 23 (2004) 2541–2547.
[3] J.A. Pedersen, Spectrochim. Acta A 58 (2002) 1257–1277.
[4] T. Yagashita, S. Sawayama, K. Tsukahara, T. Ogi, Renewable Energy 9 (1996) 958–961.
[5] G. Kreysa, D. Sell, P. Kramer, B. Bunsenges, Phys. Chem. 94 (1990) 1042–1045.
[6] S. Rane, S. Gawali, S. Padhye, S. Date, P. Bakare, Indian J. Chem. 42A (2003) 255–261.
[7] S. Salunke-Gawali, R. Dalvi, K. Ahmed, S. Rane, J. Therm. Anal. Calorim. 76 (2004) 801–812.
[8] S.I. Allakhverdiev, M.S. Karacan, G. Somer, N. Karacan, E.M. Khan, S.Y. Rane, S. Padhye, V.V. Klimov, G. Renger, Biochemistry 33 (1994) 12210–12214.
[9] S.I. Allakhverdiev, M.S. Karacan, G. Somer, N. Karacan, E.M. Khan, S.Y. Rane, S. Padhye, V.V. Klimov, G. Renger, Z. Naturforsch 49c (1994) 587–592.
[10] (a) A.V. Todkary, N.R. Dhumal, S.Y. Rane, J.V. Yakhmi, S.A. Salunke, J. Marrot, F. Varret, S.P. Gejji, Hydrogen bonding motif in 2-hydroxy-1,4-naphthoquinone: theory and experiment, in: XXXIII National Seminar on Crystallography Abstracts, N.C.L., Pune, India, 2004;
(b) N.R. Dhumal, A.V. Todkary, S.Y. Rane, S.P. Gejji, Theor. Chem. Acc. 113 (2005) 161–166.
[11] S. Salunke-Gawali, S.Y. Rane, K. Boukheddaden, E. Codjovi, J. Linares, F. Varret, P.P. Bakare, J. Therm. Anal. Calorim. 79 (2005) 669–675.
[12] S.Y. Rane, D.D. Dhavale, M.P. Mulay, E.M. Khan, Spectrochim. Acta A 46 (1990) 113.
[13] K.A. Joshi, D.R. Thube, S.Y. Rane, S.P. Gejji, Theor. Chem. Acc. 110 (2003) 322–327.
[14] D.D. Perrin, W.L. Armarego, D.R. Perrin, Purification of Laboratory Chemicals, Pergamon Press, London, 1966.
[15] S.Y. Rane, S.B. Padhye, E.M. Khan, P.L. Garge, Synth. React. Inorg. Met.-Org. Chem. 18 (1988) 609–627.
[16] G.M. Sheldrick, SADABS Program for Scaling and Correction of Area Detector Data, University of Göttingen, Göttingen (Germany), 1997;
R.H. Blessing, Acta Crystallogr. 51A (1995) 33.
[17] G.M. Sheldrick, SHELX-TL, Version 5.1, University of Göttingen, Bruker AXS Inc., Madison, WI, 1998.
[18] (a) T. Threlfall, Org. Process Res. Dev. 4 (2000) 384–390;
(b) R.K.R. Jetti, R. Boese, J.A.R.P. Sarma, L.S. Reddy, P. Vishweshwar, G.R. Desiraju, Angew. Chem. Int. Ed. Engl. 42 (2003) 1963–1967.
[19] J. Gaultier, C. Hauw, Acta Crystallogr. 19 (1965) 919–926.
[20] J. Gaultier, C. Hauw, Acta Crystallogr. 19a (1965) 580–584.
[21] J. Dekkers, H. Kooijman, J. Kroon, E. Grech, Acta. Crystallogr. C52 (1996) 2896–2899.
[22] ORTEP-III Oak Ridge, Thermal Ellipsoid Plot Program for Crystal Structure Illustrations, Oak Ridge National Laboratory Report ORNL-6895, 1996.
[23] L. Fabian, A. Kalman, Acta Crystallogr. B60 (2004) 547–558.
[24] J. Bernstein, M.D. Cohen, L. Leiserowitz, in: S. Patai, Z. Rappoport (Eds.), The Structural Chemistry of Quinones, Part-I, vol. 2, John Wiley & Sons, 1988, p. 84.
[25] T.C. Hollocher, M.M. Weber, Nature 195 (1962) 247–249.
[26] J.H. Binks, A.T. Bullock, D.J. Hopkin, J. Chem. Soc., Faraday Trans. II 68 (1972) 814–820.
[27] J.A. Pedersen, J. Chem. Soc., Perkin II (1973) 424–431.
[28] P. Ashworth, W.T. Dixon, J. Chem. Soc., Perkin II (1974) 739–744.
[29] W.T. Dixon, M. Pat, M. Kok, D. Murphy, Tetrahedron. Lett. 8 (1976) 623–626.

[30] J.A. Pedersen, Spectrochim. Acta A 58 (2002) 1257–1277.
[31] H. Rostkowska, M.J. Nowak, L. Lapinski, L. Adamowicz, Spectrochim. Acta A 54 (1998) 1091–1103.
[32] K.A. Idriss, H. Sedaira, E.Y. Hashem, M.S. Saleh, S.A. Soliman, Monatsh. Chem. 127 (1996) 29–42.
[33] N.S. Isaacs, R.D. Eldik, J. Chem. Soc., Perkin Trans. 2 (1997) 1465–1467.
[34] M.A. Brown, B.R. Mc Garvey, D.G. Tuck, J. Chem. Soc., Dalton Trans. (1998) 1371–1375.
[35] A.M. El-Hendawy, Polyhedron 10 (1991) 2511–2518.
[36] Y. Tan, F-S. Xiao, G. Zheng, K. Zhen, C. Fang, J. Mol. Catal. A 157 (2000) 65–72.
[37] J.E. Wertz, J.R. Bolton, in: Chapman, Hal (Eds.), Electron Spin Resonance—Elementary Theory and Practical Applications, N.Y., 1986.
[38] D.A. Shultz, G.T. Farmer, J. Org. Chem. 63 (1998) 6254–6257.
[39] J.F.W. Keanna, R.J. Dinerstein, J. Am. Chem. Soc. 93 (11) (1971) 2808–2810.
[40] W.H.J. Goslar, J. Trit-Goc, S.K. Hoffmann, Inorg. Chem. 34 (1995) 1852–1858.
[41] Cambridge Crystallographic Data Centre (publ. no. 212887), e-mail: deposite@ccdc.com.ac.uk.
[42] J. Bernstein, M.D. Cohen, L. Leiserowitz, in: S. Patai (Ed.), The Chemistry of the Quinonoid Compounds, John Wiley & Sons, 1974.
[43] F. Van Bolhuis, C.T. Kiers, Acta. Crystallogr. Sect. B34 (1978) 1015.
[44] C.G. Pierpont, C.W. Lange, Prog. Inorg. Chem. 41 (1994) 331.
[45] L. Que Jr., J.D. Lipscomb, E. Münck, J.M. Wood, Biochim. Biophys. Acta 485 (1977) 60.